# Photochemical Resolution of a Thermally Inert Cyclometalated Ru(phbpy)(N−N)(Sulfoxide)+ Complex

Lucien N. Lameijer,[†,§] Corjan van de Griend,[†,§] Samantha L. Hopkins,[†] Anne-Geert Volbeda,[†] Sven H. C. Askes,[†] Maxime A. Siegler,[‡] and Sylvestre Bonnet*[,†]

[†]Leiden Institute of Chemistry, Leiden University, Einsteinweg 55, 2333CC Leiden, The Netherlands
[‡]Small molecule X-ray facility, Department of Chemistry, John Hopkins University, Baltimore, Maryland 21218, United States

Ⓢ *Supporting Information*

**ABSTRACT:** In this work a photosubstitution strategy is presented that can be used for the isolation of chiral organometallic complexes. A series of five cyclometalated complexes Ru(phbpy)(N−N)(DMSO-$\kappa$S)](PF$_6$) ([**1**]PF$_6$-[**5**]PF$_6$) were synthesized and characterized, where Hphbpy = 6′-phenyl-2,2′-bipyridyl, and N−N = bpy (2,2′-bipyridine), phen (1,10-phenanthroline), dpq (pyrazino[2,3-*f*][1,10]phenanthroline), dppz (dipyrido[3,2-*a*:2′,3′-*c*]phenazine, or dppn (benzo[*i*]dipyrido[3,2-*a*,2′,3′-*c*]phenazine), respectively. Due to the asymmetry of the cyclometalated phbpy$^-$ ligand, the corresponding [Ru-(phbpy)(N−N)(DMSO-$\kappa$S)]$^+$complexes are chiral. The exceptional thermal inertness of the Ru−S bond made chiral resolution of these complexes by thermal ligand exchange impossible. However, photosubstitution by visible light irradiation in acetonitrile was possible for three of the five complexes ([**1**]PF$_6$-[**3**]PF$_6$).



Further thermal coordination of the chiral sulfoxide (*R*)-methyl *p*-tolylsulfoxide to the photoproduct [Ru(phbpy)(phen)(NCMe)]PF$_6$, followed by reverse phase HPLC, led to the separation and characterization of the two diastereoisomers of [Ru(phbpy)(phen)(MeSO(C$_7$H$_7$))]PF$_6$, thus providing a new photochemical approach toward the synthesis of chiral cyclometalated ruthenium(II) complexes. Full photochemical, electrochemical, and frontier orbital characterization of the cyclometalated complexes [**1**]PF$_6$-[**5**]PF$_6$ was performed to explain why [**4**]PF$_6$ and [**5**]PF$_6$ are photochemically inert while [**1**]PF$_6$-[**3**]PF$_6$ perform selective photosubstitution.
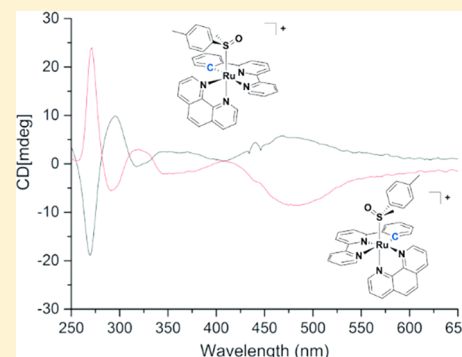
## ■ INTRODUCTION

Since the clinical approval of cisplatin a great number of inorganic complexes with anticancer properties have been described, among which several ruthenium complexes have reached clinical trials. Currently, most research is focused on either compounds based upon the piano-stool Ru(II)$\eta^6$-arene scaffold pioneered by the groups of Dyson and Sadler,[1,2] or ruthenium(II) polypyridyl complexes, of which several (photo-active) candidates have been developed by the groups of Dunbar,[3] Gasser,[4] Glazer,[5] Renfrew,[6] Keyes,[7,8] Kodanko,[9,10] or Turro.[11] More recently cyclometalated analogues of these complexes have emerged as a new subclass of light-activatable anticancer complexes.[3,12,13] In this type of compounds, one nitrogen atom in a polypyridyl ligand has been replaced by a carbon atom, resulting in an organometallic metallacycle.[14−17] As a consequence, cyclometalated compounds often show enhanced properties for chemotherapy or photodynamic therapy (PDT) than their noncyclometalated analogons.[14] In particular, the lower charge of cyclometalated complexes leads to an increased lipophilicity, which in turn increases uptake in cancer cells[18] and often leads to higher cytotoxicity[19] toward cancer cells. In addition, cycloruthenated polypyridyl complexes have increased absorption in the red region of the spectrum, which is excellent for photochemotherapy. Whereas polypyridyl ruthenium complexes typically absorb between 400

and 600 nm,[20] a bathochromic shift is usually observed for cyclometalated compounds due to the destabilization of t$_{2g}$ orbitals by the $\pi$-donating cyclometalated carbanionic ligand, potentially allowing activation of these compounds in the photodynamic window, (600−1000 nm) where light penetrates further into biological tissue.[21] Although cyclometalation often leads to a significant decrease of the photosubstitution properties of ruthenium complexes, the group of Turro has reported two cyclometalated complexes, *cis*-[Ru(phpy)(phen)-(MeCN)$_2$]PF$_6$ and *cis*-[Ru(phpy)(bpy)(MeCN)$_2$]PF$_6$, (phpy = 2-phenylpyridine), that are capable of exchanging their acetonitrile ligand upon light irradiation and are phototoxic in cancer cells.[22]

Inspired by this work and following our investigation of caged ruthenium complexes with the general formula [Ru-(tpy)(N−N)(L)]$^{2+}$ in which L is a sulfur-based ligand and tpy = 2,2′;6′,2″-terpyridine, we herein investigated the preparation and properties of cyclometalated analogues of this family of complexes where the carbanion is introduced in the tridentate ligand. Five complexes [**1**]PF$_6$−[**5**]PF$_6$ with the general formula [Ru(phbpy)(N−N)(DMSO-$\kappa$S)]PF$_6$ with Hphbpy = 6′-phenyl-2,2′-bipyridyl and N−N = bpy (2,2′-bipyridine,

[**1**]PF$_6$), phen (1,10-phenanthroline, [**2**]PF$_6$), dpq (pyrazino-[2,3-*f*][1,10]phenanthroline, [**3**]PF$_6$), dppz (dipyrido[3,2-*a*:2′,3′-*c*]phenazine), [**4**]PF$_6$), and dppn (benzo[*i*]dipyrido-[3,2-*a*:2′,3′-*c*]phenazine, [**5**]PF$_6$), respectively, were considered. Interestingly, by replacing one of the lateral nitrogen atoms of terpyridine in [Ru(tpy)(N–N)(L)]$^{2+}$ by a carbon ligand, these ruthenium complexes become chiral, and using chiral monodentate sulfoxides should allow for separating their diastereomers.[23−25] However, these cyclometalated complexes turned out to be substitutionally inert under thermal conditions, preventing displacement of DMSO in the racemic precursor. In order to achieve the resolution of [**1**]PF$_6$, it was therefore necessary to design a photochemical route. By investigating the photophysical properties and photoreactivity of these complexes, three of these complexes were found suitable for this approach, of which one was resolved using a chiral monodentate sulfoxide ligand.

## ■ RESULTS

**Synthesis and Crystal Structures.** The first attempted route toward the synthesis of compounds [**1**]PF$_6$–[**5**]PF$_6$ (Figure 1), inspired by the report of Ryabov and co-workers,[26]
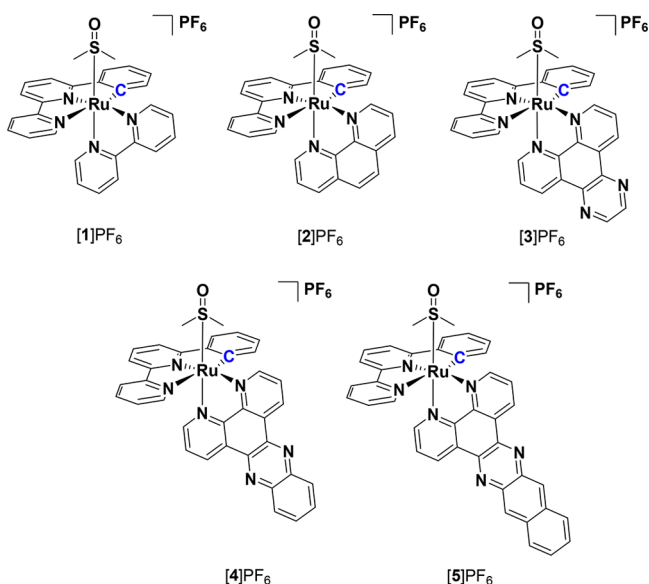


**Figure 1.** Chemical structures of the complexes presented in this study. [Ru(phbpy)(N–N)(DMSO-*κ*S)]$^+$, where N-N = bpy, phen, dpq, dppz, or dppn.

consisted of the coordination of the terpyridine analogon Hphbpy to the ruthenium benzene dimer [(η$^6$-C$_6$H$_6$)RuCl(μ-Cl)]$_2$. However, this approach afforded the intermediate species [Ru(phbpy)(MeCN)$_3$]PF$_6$ in a maximum yield of only 32% and proved to be difficult to scale up. Therefore, an alternative route depicted in Scheme 1 was developed. Starting from *cis*-[RuCl$_2$(DMSO-*κ*S)$_3$(DMSO-*κ*O)], the reaction of the bidentate ligand N−N = bpy, phen, dpq, dppz, or dppn was realized first, followed by cyclometalation using Hphbpy in the presence of a catalytic amount of *N*-methylmorpholine, affording the five compounds [Ru(phbpy)(N−N)(DMSO-*κ*S)]PF$_6$ ([**1**]PF$_6$−[**5**]PF$_6$) as a racemic mixture of enantiomers in good yield (65−74%).

Single crystals suitable for X-ray structure determination were obtained by slow vapor diffusion of ethyl acetate in dichloromethane for [**1**]PF$_6$, hexane in dichloromethane for [**2**]PF$_6$ and [**3**]PF$_6$, and toluene in DCM for [**4**]PF$_6$. All compounds crystallized in space groups having an inversion center, thus containing a (1:1) mixture of enantiomers. A selection of bond lengths and angles is shown in Table 1. As

**Table 1. Selected Bond Distances (Å) and Bond Angles (deg) for Complexes [1]PF$_6$, [2]PF$_6$, [3]PF$_6$, and [4]PF$_6$.**

|          | [**1**]PF$_6$ | [**2**]PF$_6$ | [**3**]PF$_6$ | [**4**]PF$_6$ |
|----------|-----------|-----------|-----------|-----------|
| Ru1−S1   | 2.2558(7) | 2.2359(4) | 2.2405(9) | 2.210(3)  |
| Ru1−C1   | 2.043(2)  | 2.041(3)  | 2.029(5)  | 2.030(1)  |
| Ru1−N1   | 2.002(2)  | 2.004(2)  | 2.005(5)  | 2.019(7)  |
| Ru1−N2   | 2.173(2)  | 2.164(2)  | 2.176(3)  | 2.180(1)  |
| Ru1−N3   | 2.088(2)  | 2.110(2)  | 2.089(3)  | 2.094(3)  |
| Ru1−N4   | 2.079(2)  | 2.091(2)  | 2.083(4)  | 2.071(4)  |
| S1−O1    | 1.486(2)  | 1.489(2)  | 1.485(3)  | 1.501(6)  |
| C1−Ru1−N2 | 157.92(8) | 158.45(9) | 158.5(2)  | 155.6(7)  |
| N3−Ru1−N4 | 78.07(7) | 78.67(7)  | 78.9(1)   | 78.2(1)   |
| S1−Ru1−N4 | 96.25(5) | 97.29(5)  | 96.6(1)   | 96.0(1)   |

expected, the ruthenium centers in these compounds have a distorted octahedral geometry similar to that of their terpyridyl analogues.[27] Compared to [Ru(tpy)(bpy)(DMSO-*κ*S)](OTf)$_2$ replacing the nitrogen within this scaffold with an anionic carbon atom has only a modest effect on the corresponding bond length, with Ru1−C1 in [**1**]PF$_6$ (2.043(2) Å) being almost as long as Ru1−N1 in its terpyridine analogue (2.079 Å).[28] Furthermore, compared to its noncyclometalated analogon the trans-influence of the carbon atom in phbpy$^−$ results in an elongation of the Ru1−N2 bond length in [Ru(phbpy)(bpy)(DMSO-*κ*S)]$^{2+}$ (2.173(2) Å), whereas in [Ru(tpy)(bpy)(DMSO-*κ*S)]$^{2+}$ the Ru1−N3 length is 2.073(3) Å.[29] In contrast, the ruthenium−sulfur bond length is shorter

**Scheme 1. Reagents and Conditions$^a$**
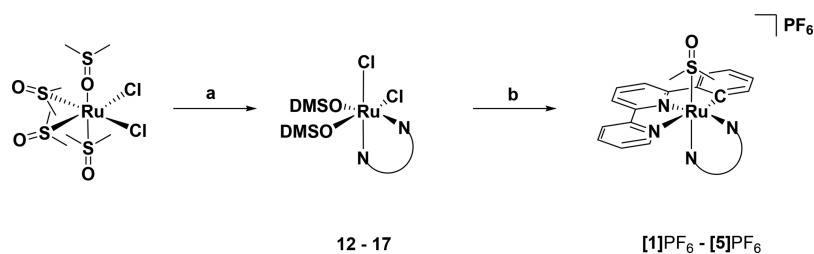


$^a$(a) N−N = bpy in EtOH/DMSO (15:1), reflux, 86%; (b) HPhbpy, cat. *N*-methylmorpholine in MeOH/H$_2$O (5:1), reflux, 65%. For N−N = phen = 77% and 68%, N−N = dpq = 95% and 74%, N−N = dppz = 87% and 73%, NN = dppn = 96% and 65%.
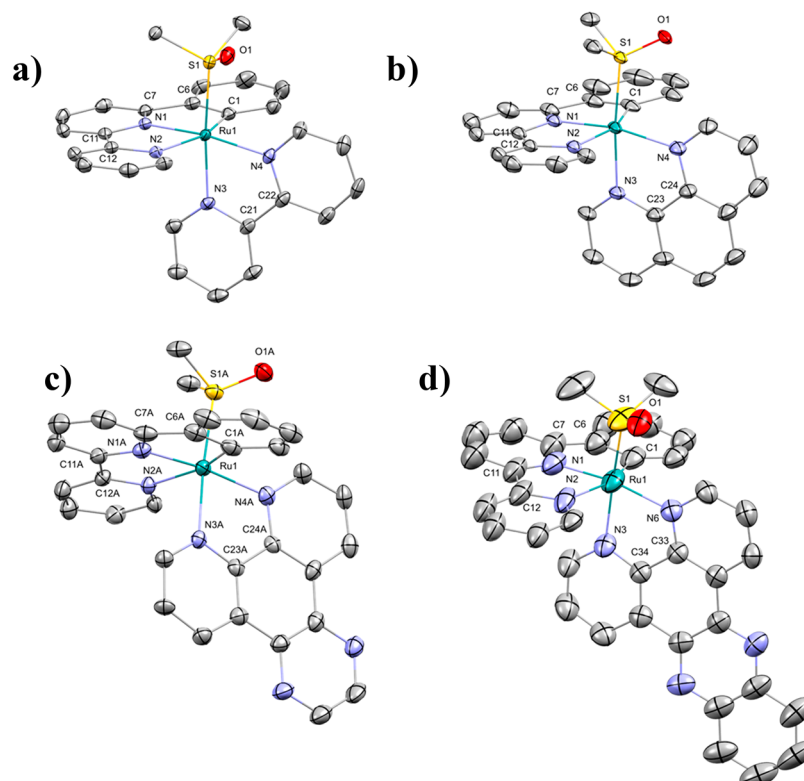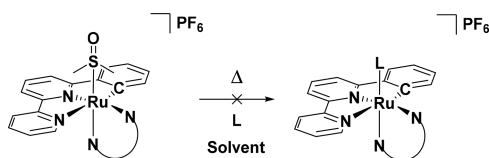
**Figure 2.** Displacement ellipsoid plots (50% probability level) of the cationic part of the crystal structure of [1]PF$_6$ (a), [2]PF$_6$ (b), [3]PF$_6$ (c), and [4]PF$_6$ (d). Hydrogen atom and counterions have been omitted for clarity.

in [1]PF$_6$ (2.2558(7) Å) than in [Ru(tpy)(bpy)(DMSO-κS)]$^{2+}$ (2.282(1) Å) as a result of the increased electron density on ruthenium, leading to stronger backbonding into the π* orbital of the S-bound DMSO ligand. Overall, this electronic effect barely affects the angles between C1−Ru1−N3 for [1]PF$_6$ (158.67(12) Å) and N1−Ru1−N3 for [Ru(tpy)(bpy)(DMSO-κS)]$^{2+}$ (157.92(8) Å), confirming their high structural similarity (Figure 2).

**Thermal Stability.** With compounds [1]PF$_6$−[5]PF$_6$ in hand, we first attempted to obtain diastereomers by the thermal reaction of several chiral ligands as shown in Scheme 2 and summarized in Table 2 (entries 1−6). Heating [1]PF$_6$ and (R)-methyl p-tolylsulfoxide at increased temperatures (up to 120 °C) in DMF resulted in the formation of ruthenium(III) species, as observed by a green color, whereas lower temperatures only led to the recovery of starting materials. Further attempts to substitute the monodentate ligand with nonchiral ligands (entries 7 and 8) such as LiCl, pyridine, or acetonitrile also proved to be unsuccessful. This thermal inertness was highly unexpected, since terpyridine analogues of these complexes are known to readily exchange their monodentate ligand in similar or much milder conditions.[30]
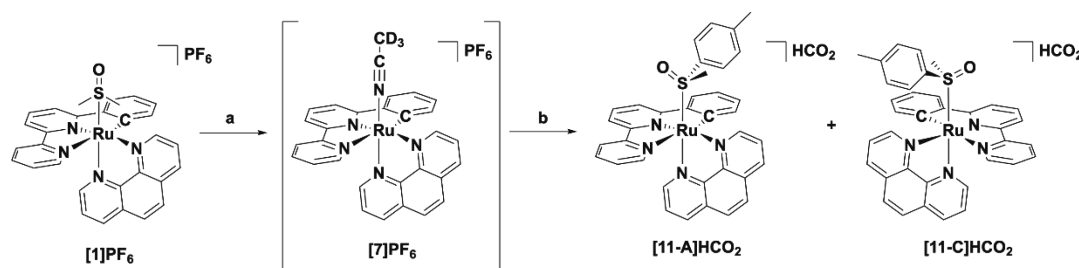
The only thermal substitution possible, observed with [4](PF$_6$)$_2$, was obtained by prolonged heating (16 h) in acetic acid, which resulted in the partial formation of [Ru(phbpy)-(dppz)(AcOH)]$^+$ as proven by mass spectrometry (found m/z 675.1, calcd. m/z 675.1). However, this species could not be isolated. Overall, the exceptional thermal inertness of the DMSO ligand in [1]PF$_6$−[5]PF$_6$ required the development of an alternative strategy for the resolution of this family of chiral complexes.

**Photosubstitution.** Replacing the DMSO ligands in these complexes was therefore attempted photochemically, monitoring the reaction using $^1$H NMR. When a sample of [2]PF$_6$ was irradiated in acetonitrile with white light (hν ≥ 410 nm, Scheme 3), a clean photoconversion to a new species was observed, which was confirmed to be the acetonitrile adduct by mass spectrometry. As shown in Figure 3, the $^1$H NMR spectra clearly demonstrate the formation of the single species [Ru(phbpy)(phen)(MeCN)]$^+$ ([7]$^+$) characterized by a doublet appearing at 9.88 ppm, while the doublet of the starting material at 10.49 ppm quantitatively disappeared. This photochemical behavior is comparable to the photosubstitution occurring in [Ru(tpy)(N−N)(X)]$^{2+}$.[31] In a similar fashion, the DMSO ligand in [1]PF$_6$ and [3]PF$_6$ could also be exchanged upon photoirradiation by deuterated acetonitrile to afford [Ru(phbpy)(bpy)(CD$_3$CN)]$^+$ ([6]$^+$) and [Ru-(phbpy)(dpq)(CD$_3$CN)]$^+$ ([8]$^+$), respectively. However, [4]PF$_6$ and [5]PF$_6$ were not photosubstitutionally active, in contrast to the noncyclometalated analogons [Ru(tpy)(dppz)-(SRR′)] and [Ru(tpy)(dppn)(SRR′)] (SRR′ = 2-(2-(2-(methylthio)ethoxy)ethoxy)ethyl-β-D-glucopyranoside)[27] that both exchange their thioether ligand upon light irradiation.[27]

**Resolving Diastereomers.** The photoactivity of [1]PF$_6$−[3]PF$_6$ therefore allowed us to investigate separation of their

**Scheme 2. General Approach for the Thermal Conversion of Complexes [1]PF$_6$, [2]PF$_6$, and [4]PF$_6$ with Different Monodentate Ligands L**

## Table 2. Attempts of Ligand Exchange for [1]PF$_6$, [2]PF$_6$, and [4]PF$_6$

| entry | complex | ligand (L) | solvent | T (°C) | substitution | reaction time (h) |
|---|---|---|---|---|---|---|
| 1 | [1]PF$_6$ | (R)-methyl p-tolylsulfoxide (5 equiv) | DMF | 120 | | 16 |
| 2 | [1]PF$_6$ | (R)-methyl p-tolylsulfoxide (5 equiv) | DMF | 80 | | 16 |
| 3 | [1]PF$_6$ | (R)-methyl p-tolylsulfoxide (5 equiv) | EtOH 3:1 H$_2$O | 80 | | 16 |
| 4 | [4]PF$_6$ | biotin (20 equiv) | EtOH 3:1 H$_2$O | 80 | | 16 |
| 5 | [4]PF$_6$ | N-acetyl-L-methionine (20 equiv) | EtOH 3:1 H$_2$O | 80 | | 16 |
| 6 | [4]PF$_6$ | N-acetyl-L-cysteine methyl ester (20 equiv) | EtOH 3:1 H$_2$O | 80 | | 16 |
| 7 | [4]PF$_6$ | L-histidine methyl ester 2HCl (20 equiv) | EtOH 3:1 H$_2$O | 80 | | 16 |
| 8 | [2]PF$_6$ | LiCl (20 equiv) | EtOH 3:1 H$_2$O | 80 | | 16 |
| 9 | [4]PF$_6$ | | MeCN | 80 | | 16 |
| 10 | [4]PF$_6$ | | pyridine | 80 | | 16 |
| 11 | [4]PF$_6$ | | acetic acid | 80 | yes | 16 |

## Scheme 3. Reagents and Conditions for the Synthesis of [11-A/C]HCO$_2$[a]



[a](a) $h\nu \geq 410$ nm in CD$_3$CN. (b) i. (R)-Methyl p-tolylsulfoxide in MeOH, reflux, 16 h; ii. Reverse-phase HPLC (0.1% HCO$_2$H in MeCN/H$_2$O). (5% over two steps for [11-A]HCO$_2$, 4% over two steps for [11-C]HCO$_2$).
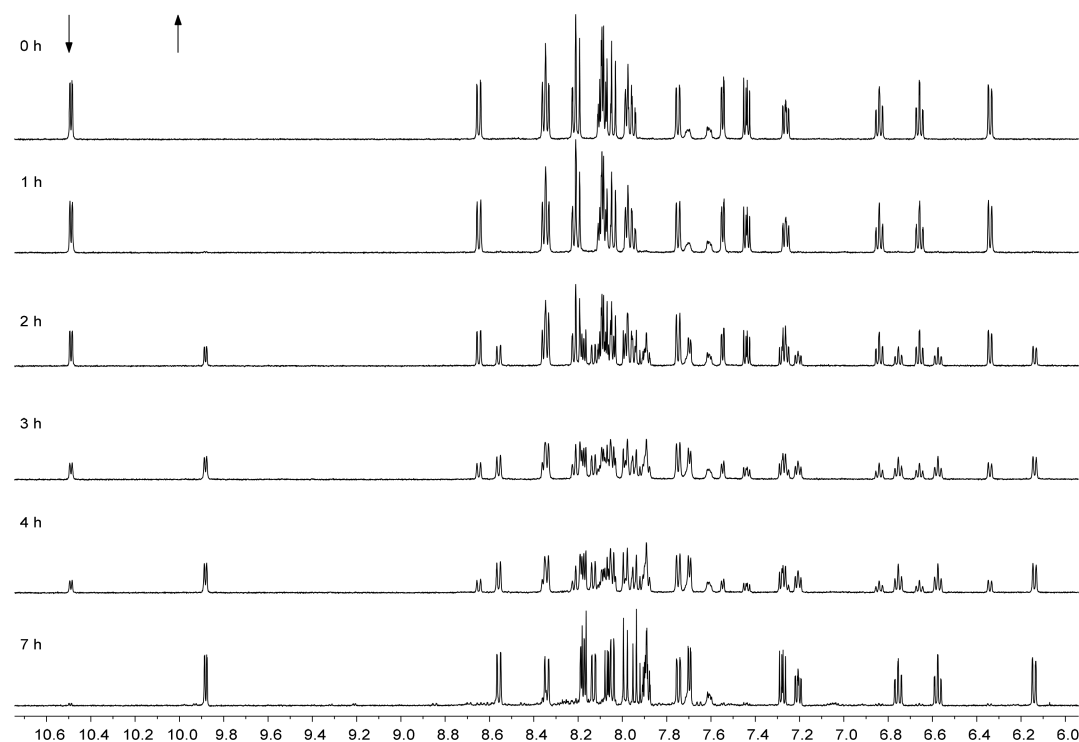


**Figure 3.** Evolution of the $^1$H NMR spectra of [2]PF$_6$ in CD$_3$CN (3.0 mg in 0.6 mL) upon irradiation with white light (>410 nm) from a 1000 W xenon Arc lamp fitted with 400 nm cutoff filter 1 cm from the light source at $T$ = 298 K. Spectra were taken every 1 h, with $t_{irr}$ = 7 h.

enantiomers. [2]PF$_6$ was used as representative example. In a first attempt, [2]PF$_6$ was converted to [7]PF$_6$ using white light irradiation in deuterated acetonitrile (~7 h). However, neither chiral HPLC nor crystallization using sodium (+)-tartrate allowed for resolving this intermediate. Instead, an alternative approach was used: racemic [7]PF$_6$ was allowed to react with an excess of enantiomerically pure (R)-methyl p-tolylsulfoxide in MeOH, affording a (1:1) mixture of diastereomers of (anticlockwise/clockwise) A/C-[Ru(phbpy)(phen)(R)-Methyl p-tolylsulfoxide)]PF$_6$, [11-A/C]HCO$_2$ (Scheme 3). Sub-
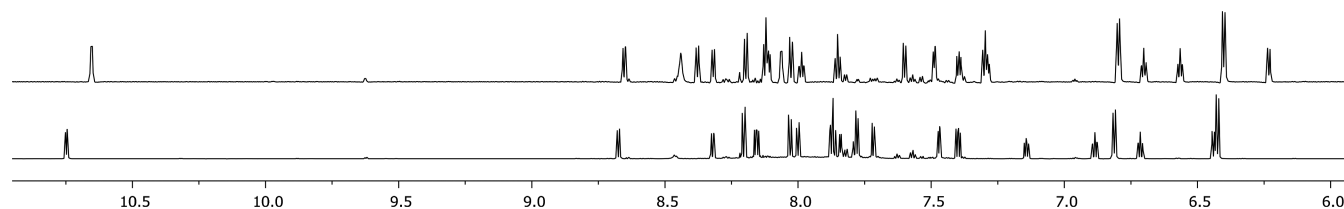
**Figure 4.** $^1$HNMR spectrum (850 MHz) of [11-C]PF$_6$ (top) and [11-A]PF$_6$ (bottom).

sequent purification over a reverse phase HPLC column afforded [11-A]HCO$_2$ and [11-C]HCO$_2$ as their respective diastereomers in 9% yield (5% over two steps for [11-A]HCO$_2$ and 4% over two steps for [11-C]HCO$_2$ (Figure S6). $^1$H NMR confirmed that fraction 1 corresponded to the R-C diastereomer, which is most apparent because of its more shielded $\alpha$-proton of phen appearing at 10.64 ppm (Figure 4). Fraction 2 contained the R-A diastereomer, with a doublet appearing at 10.74 ppm (Figure 4). This deshielding effect on the $\alpha$-proton on phen is most likely attributed to the interaction of the tolyl group with the bidentate ligand. This assumption was supported by NOESY experiments (Figure S8), which showed the absence of interaction between the methyl of the sulfoxide and phen, whereas a weak interaction was observed for [11-A]HCO$_2$ (Figure S8). Both [11-A]HCO$_2$ and [11-C]PF$_6$ are diastereomers and not enantiomers, so that specific rotation would not give any valuable information on their chirality. Circular dichroism (CD) was used instead to demonstrate they are related to the two enantiomers [2-A]$^+$ and [2-C]$^+$. The CD spectra of [11-A]PF$_6$ and [11-C]PF$_6$ in MeCN (Figure 5) displayed
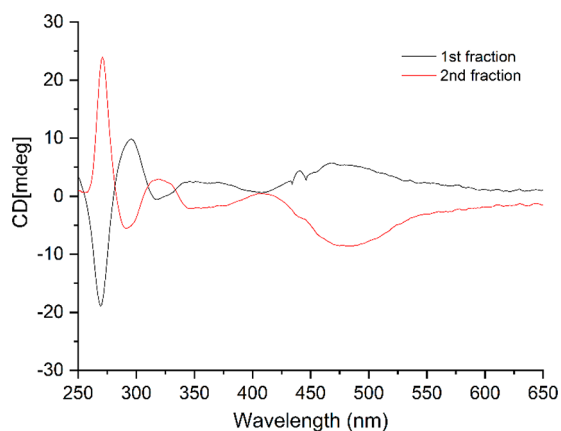


**Figure 5.** Superposition of CD spectra of first fraction (black, [11-C]HCO$_2$) and second fraction (red, [11-A]HCO$_2$) eluted diastereoisomers. $T = 293$ K, $c = 5 \times 10^{-5}$ M in MeCN.

symmetrical curves typical for enantiomers, except in the region below 250 nm where the contribution of the chiral (R)-tolylsulfoxide ligand to the absorption becomes non-negligible.[32] Around 450 nm, either positive or negative Cotton effects were observed for [11-A]PF$_6$ or [11-C]PF$_6$, respectively, which must originate from the $^1$MLCT transitions. Theoretically, resolution of these complexes by performing blue light irradiation in acetonitrile may be tempting. However, photosubstitution is usually accompanied by racemization of the coordination sphere, so that thermal ligand substitution would be preferred.[33] This was however not possible due to the exceptional thermal stability of the

sulfoxide cyclometalated complexes (see above) that prevented thermal displacement of the chiral sulfoxide to obtain isolated enantiomers of [A-7]$^+$, [C-7]$^+$, [A-2]$^+$, or [C-2]$^+$. However, the mirrored CD spectra of the diastereoisomers [11-A]HCO$_2$ and [11-C]HCO$_2$ provided a clear proof of the opposite chirality of these complexes.

**Photophysical and Photochemical Characterization.** The difference in photoreactivity between [1]$^+$–[3]$^+$ and [4]$^+$–[5]$^+$ was not straightforward to understand, and therefore a full photophysical characterization of the five complexes was carried out. The electronic absorption spectra (Figure S1) of these complexes show that they have a considerable bathochromic shift (~40 nm, Table 3) and a significant broadening of their $^1$MLCT band compared to [9]$^{2+}$ (411 nm, Table 3). [4]$^+$ and [5]$^+$ have additional absorption bands around 370 and 410 nm, respectively. These are most likely $\pi$–$\pi$* transitions arising from the dppz and dppn ligand. The spectra of [6]$^+$–[8]$^+$ in acetonitrile also showed a shift of the $^1$MLCT band of ~50 nm compared to [10]$^{2+}$. This bathochromic shift is common for cyclometalated ruthenium complexes[12,34] and is mostly ascribed to an increase in the energy of the highest occupied molecular orbital (HOMO, t$_{2g}$).[12]

Visible light excitation of ruthenium polypyridyl complexes typically leads to (1) ligand exchange, (2) phosphorescence and/or, (3) singlet oxygen generation. First, the ability of [1]PF$_6$–[5]PF$_6$ to exchange the DMSO ligand for a solvent molecule was quantified by UV–vis spectroscopy (Figure 6). As observed under white light irradiation (>450 nm), monochromatic blue light irradiation in acetonitrile (450 nm) left [4]PF$_6$ and [5]PF$_6$ unaffected, while [1]PF$_6$–[3]PF$_6$ converted to the acetonitrile complexes [6]PF$_6$–[8]PF$_6$ with clear isosbestic points (441 and 490 nm for [1]PF$_6$, 470 nm for [2]PF$_6$, and 455 nm for [3]PF$_6$) confirming the selectivity of the photoconversion. ESI-MS spectra taken after each reaction confirmed the formation of the acetonitrile photoproducts. The photosubstitution quantum yields ($\Phi_{450}$) were found to be $4.1 \times 10^{-5}$ for [1]PF$_6$, $1.3 \times 10^{-5}$ for [2]PF$_6$, and $2.2 \times 10^{-5}$ for [3]PF$_6$, which is a thousand times lower than that measured for [Ru(tpy)(bpy)(DMSO-$\kappa$S)]$^{2+}$($\Phi_{450} = 1.6 \times 10^{-2}$). This decreased reactivity is most likely caused by the destabilization of the $^3$MC state due to increased electron density at the metal center brought by the strong $\sigma$-donor C atom, whereas stabilization of the $^3$MLCT leads to a larger energy gap between the $^3$MLCT and $^3$MC state, therefore making thermal population of the latter rather unlikely.[34] This interpretation is supported by previous work of the Turro group, who has demonstrated that the efficiency of the photosubstitution in sterically congested cyclometalated complexes is very low or absent.[12,22]

Second, emission maxima ($\lambda_{em}$) and emission quantum yields ($\Phi_P$) for [1]PF$_6$–[5]PF$_6$ were measured in acetonitrile (Table 3). All compounds were found very weakly emissive

**Table 3. Lowest-Energy Absorption Maxima ($\lambda_{max}$), Molar Absorption Coefficients at $\lambda_{max}$ ($\varepsilon$ in M$^{-1}$ cm$^{-1}$), Photosubstitution Quantum Yields in Acetonitrile ($\Phi_{450}$) at 298 K, $^1O_2$ Quantum Yields ($\Phi_\Delta$) at 293 K, and Phosphorescence Quantum Yield ($\Phi_P$) for [1]PF$_6$−[10](PF$_6$)$_2$**

| complex | formula | $\lambda_{max}$ ($\varepsilon_{max}$ in M$^{-1}$ cm$^{-1}$)[a] | $\lambda_{em}$ (nm) | $\Phi_\Delta$[b] | $\Phi_P$[b] | $\Phi_{450}$ |
|---|---|---|---|---|---|---|
| [1]PF$_6$ | [Ru(phbpy)(bpy)(DMSO-$\kappa S$)]PF$_6$ | 476 (50 × 10$^2$) | 786 | 3.2 × 10$^{-2}$ | 1.6 × 10$^{-4}$ | 4.1 × 10$^{-5}$ |
| [2]PF$_6$ | [Ru(phbpy)(phen)(DMSO-$\kappa S$)]PF$_6$ | 450 (57 × 10$^2$) | 800 | 3.9 × 10$^{-2}$ | 2.1 × 10$^{-4}$ | 1.3 × 10$^{-5}$ |
| [3]PF$_6$ | [Ru(phbpy)(dpq)(DMSO-$\kappa S$)]PF$_6$ | 451 (83 × 10$^2$) | 787 | 1.1 × 10$^{-1}$ | 2.1 × 10$^{-4}$ | 2.2 × 10$^{-5}$ |
| [4]PF$_6$ | [Ru(phbpy)(dppz)(DMSO-$\kappa S$)]PF$_6$ | 450 (84 × 10$^2$) | 618 | 7.0 × 10$^{-3}$ | 2.6 × 10$^{-4}$ | <10$^{-6}$ |
| [5]PF$_6$ | [Ru(phbpy)(dppn)(DMSO-$\kappa S$)]PF$_6$ | 450 (75 × 10$^2$) | 672 | <10$^{-3}$ | 8.4 × 10$^{-5}$ | <10$^{-6}$ |
| [6]PF$_6$ | [Ru(phbpy)(bpy)(CD$_3$CN)]PF$_6$ | 525 (71 × 10$^2$) | n.d. | n.d. | n.d. | |
| [7]PF$_6$ | [Ru(phbpy)(phen)(CD$_3$CN)]PF$_6$ | 503 (63 × 10$^2$) | n.d. | n.d. | n.d. | |
| [8]PF$_6$ | [Ru(phbpy)(dpq)(CD$_3$CN)]PF$_6$ | 495 (119 × 10$^2$) | n.d. | n.d. | n.d. | |
| [9](PF$_6$)$_2$ | [Ru(tpy)(bpy)(DMSO-$\kappa S$)](PF$_6$)$_2$ | 411 (75 × 10$^2$) | n.d. | n.d. | n.d. | 1.6 × 10$^{-2}$ |
| [10](PF$_6$)$_2$ | [Ru(tpy)(bpy)(MeCN)](PF$_6$)$_2$ | 455 (91 × 10$^2$) | n.d. | n.d. | n.d. | |

[a]In MeCN. [b]in CD$_3$OD.
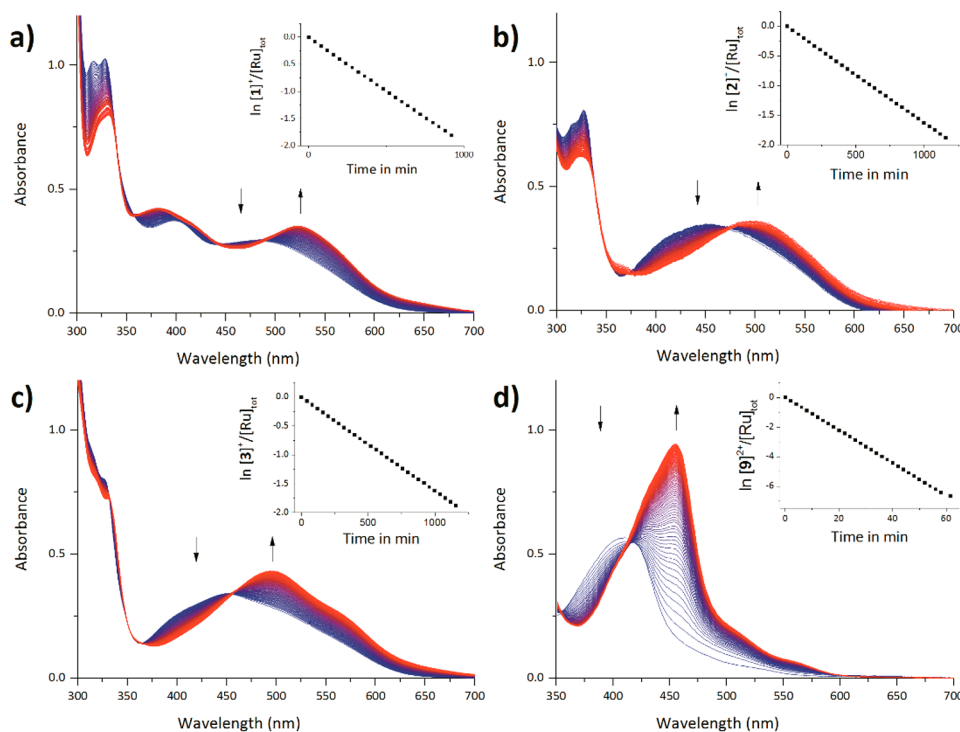


**Figure 6.** Time evolution of the electronic absorption spectra of [1]PF$_6$−[3]PF$_6$ and [9](PF$_6$)$_2$ in deoxygenated MeCN upon irradiation at 450 nm at $T$ = 298 K. Spectra measured every 30 min (every 0.5 min for [9]PF$_6$). (a) [1](PF$_6$) $t_{irr}$ = 16 h, [Ru]$_{tot}$ = 5.78 × 10$^{-5}$ M, photon flux = 1.68 × 10$^{-7}$ mol s$^{-1}$. (b) [2](PF$_6$), $t_{irr}$ = 23 h, [Ru]$_{tot}$ = 6.08 × 10$^{-5}$ M, photon flux = 1.67 × 10$^{-7}$ mol s$^{-1}$. (c) [3]PF$_6$, $t_{irr}$ = 16 h, [Ru]$_{tot}$ = 4.06 × 10$^{-5}$ M, photon flux = 1.68 × 10$^{-7}$ mol s$^{-1}$. (d) [9](PF$_6$)$_2$, $t_{irr}$ = 1 h, [Ru]$_{tot}$ = 6.52 × 10$^{-5}$ M, photon flux = 5.54 × 10$^{-8}$ mol s$^{-1}$.

with a slightly higher phosphorescence quantum yield compared to the polypyridyl complex [Ru(phbpy)(tpy)]$^+$ ($\Phi_P$ = 5 × 10$^{-6}$).[35] The emission wavelengths found for [1]$^+$−[3]$^+$ are comparable to those of [Ru(phbpy)(tpy)]$^+$ (786−800 nm versus 797 nm)[35] and are similar to complexes reported by the group of Turro and Sauvage.[12,35] For complexes [4]$^+$ and [5]$^+$ a blue-shifted emission (618 and 672 nm) was observed compared to [Ru(phbpy)(tpy)]$^+$, which suggested a different type of excited state compared to [1]$^+$−[3]$^+$. Third, singlet oxygen quantum yields ($\Phi_\Delta$) were determined in deuterated methanol by measuring the emission of $^1O_2$ at 1270 nm. $\Phi_\Delta$ values lower than 0.04 were found for all complexes with the exception of [3]PF$_6$, which produced $^1O_2$ with a photoefficiency ($\Phi_\Delta$) of 0.11. Interestingly, [Ru(phbpy)(dppn)(DMSO-$\kappa S$)]$^+$ did not show any singlet oxygen production, whereas its noncyclometalated analogues

[Ru(tpy)(dppn)(CD$_3$OD)]$^{2+}$ and [Ru(tpy)(dppn)(py)]$^{2+}$ both have been demonstrated to be excellent $^1O_2$ generators.[36,37] Overall, changing terpyridine into phenylbipyridine had great consequences on the photochemical and photophysical properties of this series of complexes. Therefore, to further understand the photophysical differences between complexes [1]$^+$−[3]$^+$ and [4]$^+$−[5]$^+$ electrochemical studies and DFT calculations were carried out.

**Electrochemistry and DFT.** The electrochemical properties of complexes [1]PF$_6$−[7]PF$_6$ and [9](PF$_6$)$_2$−[10](PF$_6$)$_2$ were determined with cyclic voltammetry (Figure 7 and Table 4) to provide insight into the frontier orbitals of the cyclometalated complexes.[38] As summarized in Table 4, the cyclometalated DMSO complexes [1]PF$_6$−[5]PF$_6$ show quasi-reversible oxidation processes ($I_{pa}/I_{pc} \approx 1$) with Ru$^{III}$/Ru$^{II}$ couples near ~+0.30 V vs Fc$^{0/+}$ whereas [9](PF$_6$)$_2$ showed an
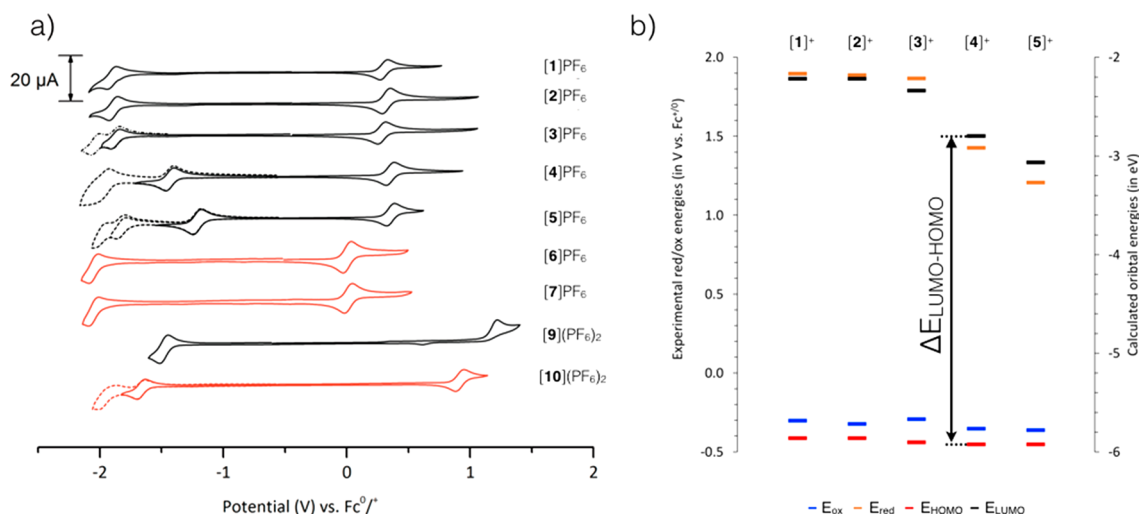
**Figure 7.** (a) Cyclic voltammograms of cyclometalated complexes [1]PF$_6$–[7]PF$_6$ and noncyclometalated complexes [9](PF$_6$)$_2$ and [10](PF$_6$)$_2$. Scan rate 100 mV s$^{-1}$, with the exception of [4]PF$_6$, [6]PF$_6$, [7]PF$_6$, and [9]PF$_6$ which were measured at 200 mV s$^{-1}$. L = DMSO-$\kappa$S or CD$_3$CN. (b) Experimental ($E_{ox}$ and $E_{red}$ from cyclic voltammetry, in V vs. Fc$^{+/0}$, left axis) and calculated (from DFT, in eV, right axis) values of the HOMO energy, LUMO energy, and $\Delta E$ energy gap.

**Table 4. Electrochemical Properties As Measured with Cyclic Voltammetry and Theoretical HOMO − LUMO Gaps Calculated by DFT**[a]

| | | $E_{ox}$ (V) | $I_{pa}/I_{pc}$ | $E_{red}$ (V) | $I_{pc}/I_{pa}$ | $\Delta E_{exp}$ (V)[c] | $\Delta E_{th}$ (eV)[d] |
|---|---|---|---|---|---|---|---|
| [Ru(phbpy)(bpy)(DMSO-$\kappa$S)]PF$_6$ | [1]PF$_6$ | +0.30 | 0.99 | −1.90 | 1.47 | 2.20 | 3.65 |
| [Ru(phbpy)(phen)(DMSO-$\kappa$S)]PF$_6$ | [2]PF$_6$ | +0.32 | 1.02 | −1.89 | 1.11 | 2.21 | 3.65 |
| [Ru(phbpy)(dpq)(DMSO-$\kappa$S)]PF$_6$ | [3]PF$_6$ | +0.29 | 1.01 | −1.87, −1.95 | 0.66, 2.23 | 2.16 | 3.57 |
| [Ru(phbpy)(dppz)(DMSO-$\kappa$S)]PF$_6$ | [4]PF$_6$ | +0.35 | 1.04 | −1.43, −2.00 | 1.03 | 1.78 | 3.13 |
| [Ru(phbpy)(dppn)(DMSO-$\kappa$S)]PF$_6$ | [5]PF$_6$ | +0.36 | 1.05 | −1.21, −1.82, −2.01 | 1.07, 1.52 | 1.57 | 2.86 |
| [Ru(phbpy)(bpy)(CD$_3$CN)]PF$_6$ | [6]PF$_6$ | 0.00 | 1.00 | −2.05 | 1.34 | 2.05 | |
| [Ru(phbpy)(phen)(CD$_3$CN)]PF$_6$ | [7]PF$_6$ | +0.02 | 1.04 | −2.05 | 1.38 | 2.07 | |
| [Ru(tpy)(bpy)(DMSO)](PF$_6$)$_2$ | [9](PF$_6$)$_2$ | +1.23[b] | | −1.48 | 1.00 | 2.71 | |
| [Ru(tpy)(bpy)(MeCN)](PF$_6$)$_2$ | [10](PF$_6$)$_2$ | +0.92 | 0.95 | −1.67 | 1.06 | 2.59 | 4.12 |

[a]Potentials given vs. Fc$^0$/Fc$^+$ in MeCN with 0.1 M [Bu$_4$N]PF$_6$ as supporting electrolyte. Complexes were measured at 298 K with a scan rate of 100 mV s$^{-1}$, with the exception of [4]PF$_6$, [6]PF$_6$ [7]PF$_6$, and [9]PF$_6$ which were measured at 200 mV s$^{-1}$. [b]$E_{pa}$. [c]$\Delta E_{th} = E_{LUMO} − E_{HOMO}$ at the DFT/PBE0/TZP/COSMO level in water. [d]$\Delta E_{exp} = E_{ox} − E_{red}$.

irreversible Ru$^{II}$ → Ru$^{III}$ oxidation at +1.23 V vs Fc$^{0/+}$. Although the irreversibility of the oxidation of [9](PF$_6$)$_2$ does not strictly speaking allow to analyze this oxidation potential to a HOMO energy level, for [1]PF$_6$–[5]PF$_6$ the low-lying, reversible oxidation suggests that the Ru(d$\pi$)-based HOMO of the cyclometalated complexes is very high in energy, due to the $\pi$-donating character of the phbpy$^-$ ligand.[12] As the irreversibility of the oxidation of [9](PF$_6$)$_2$ is attributed to linkage isomerization of DMSO from S-bound to O-bound,[39] cyclometalation also appears to prevents redox-induced linkage isomerization of the DMSO ligand, most likely due to the increased electron density on ruthenium. The quasi-reversible Ru$^{III/II}$ couple of the DMSO complexes [1]PF$_6$–[2]PF$_6$ also appeared at a higher potential (+0.30 V vs Fc$^{0/+}$) compared to that of the acetonitrile compounds [6]PF$_6$–[7]PF$_6$ (0.00 V vs Fc$^{0/+}$), which can be explained by the electronic effects of the monodentate ligand; $\kappa$S-DMSO is a stronger $\pi$-acceptor than CD$_3$CN and therefore has a stronger electron withdrawing effect on ruthenium(II).[40] The ligand-based reductions for [1]PF$_6$–[3]PF$_6$ was found to have very similar energies, with quasi-reversible reductions around −2.0 V vs Fc$^{+/0}$, suggesting that these are phbpy-based. For [4]PF$_6$ and [5]PF$_6$ however the L$^{0/-}$ appeared to occur at much less negative potentials

(−1.4 V vs Fc$^{+/0}$ for [4]PF$_6$ and −1.2 V vs Fc$^{+/0}$ for [5]PF$_6$) due to the strong electron-accepting properties of the dipyridophenazine moieties. These first reductions being essentially reversible, the LUMO of these two complexes is dppz- or dppn-based, respectively.[41] The experimental HOMO − LUMO gaps $\Delta E_{exp}$, which can be approximated, for quasi-reversible redox couples, to the difference between $E_{ox}$ and $E_{red}$ (Figure 7, left), followed similar trends to the theoretical HOMO − LUMO gaps $\Delta E_{th}$ calculated by DFT (Table 4). $\Delta E_{th}$ were found very comparable indeed for complexes [1]PF$_6$–[3]PF$_6$ ($\Delta E_{exp} \approx 2.2$ V and $\Delta E_{th} \approx 3.6$ V) and much higher than that of [4]PF$_6$ and [5]PF$_6$ ($\Delta E_{exp} = 1.8$ and 1.6 V, respectively, and $\Delta E_{th} = 3.13$ and 1.86 V). The particularly low value of $\Delta E$ found for [4]PF$_6$ and [5]PF$_6$ suggested that the dppz and dppn ligands may generate low-lying excited states, which would explain the absence of photosubstitution with these two complexes.

To confirm this hypothesis, density functional theory (DFT) calculations were performed for [1]$^+$–[5]$^+$ at the PBE0/TZP/COSMO level. The calculated HOMO energy, LUMO energy, and $\Delta E_{th} = E_{LUMO} − E_{HOMO}$ of the minimized geometries followed the same trend as the experimental values (Table 4 and Figure 7b). For [1]$^+$ and [2]$^+$ the LUMO was located on
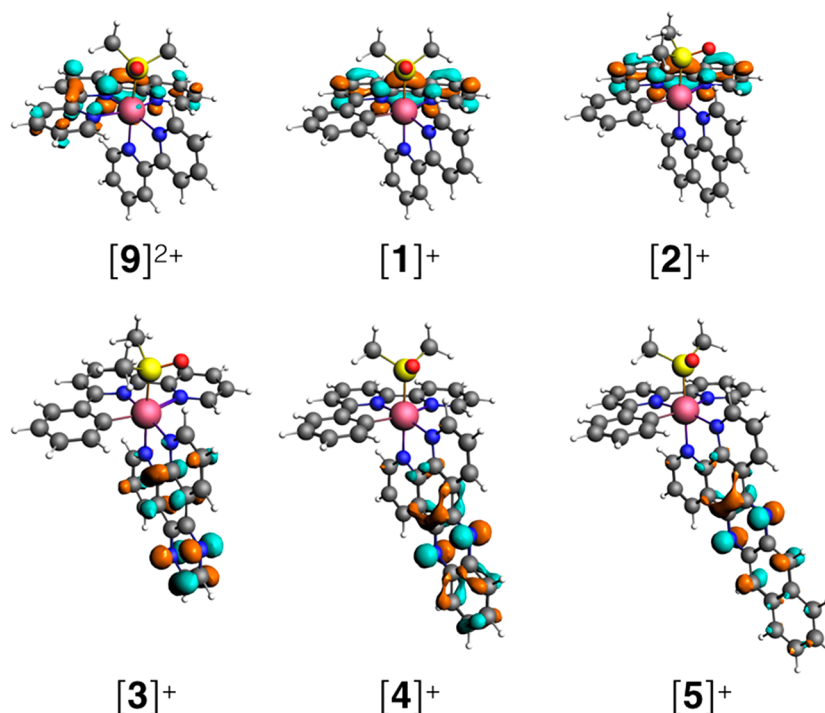
**Figure 8.** LUMO orbitals for $[Ru(tpy)(bpy)L]^{2+}$ ($[9]^{2+}$) and for $[1]^{+}-[5]^{+}$ at the DFT/PBE0/TZP/COSMO level in water.

the phbpy⁻ ligand, for $[4]^{+}$ and $[5]^{+}$ it was localized on the dppz and dppn bidentate ligand, respectively (Figure S3–5), whereas for $[3]^{+}$ empty orbitals localized both on phbpy⁻ and dpq were found close in energy and near the LUMO level. Thus, like for the terpyridine series,[41] extending the conjugation of the bidentate ligand in the cyclometalated series $[1]^{+}$ to $[5]^{+}$ resulted in a strong stabilization of the LUMO in $[4]^{+}$ and $[5]^{+}$, and in a shift of its localization, from the tridentate ligand in $[1]^{+}$ and $[2]^{+}$ to the bidentate ligand in $[4]^{+}$ and $[5]^{+}$, with $[3]^{+}$ as borderline species (Figure 7b). The strong stabilization of the LUMO in $[4]^{+}$ and $[5]^{+}$ generates low-lying excited states, most likely of $^3\pi-\pi^*$ character.

**Discussion.** Recent examples of the group of Turro have shown that complexes such as $cis$-$[Ru(phpy)(phen)(CH_3CN)_2]PF_6$ are as photoactive as their noncyclometalated counterparts, with a reported photosubstitution quantum yield ($\Phi_P$) of 0.25 in dichloromethane.[22] A more recent report by Albani et al. has shown that for $[Ru(biq)_2(phpy)]PF_6$ the phpy⁻ ligand increases the energy of the $^3MC$ state, which in their case completely prevents photodissociation of the bidentate biq ligand.[12] In the family of complexes $[1]^{+}-[5]^{+}$ presented here (Figure 8), cyclometalation of the terpyridine ligand allows photoinduced ligand exchange for three of the five complexes ($[1]^{+}-[3]^{+}$), while it is absent in the more conjugated analogues $[4]^{+}$ and $[5]^{+}$. The photoreactivity of ruthenium complexes is result of a delicate interplay of excited states of different natures and energies. In $[1]^{+}$, $[2]^{+}$, and $[3]^{+}$ the emission maximum was close to 800 nm, irrespective of the nature of the bidentate ligand, because the $^3MLCT$ excited states must be located on the phbpy ligand. By contrast, in the more conjugated complexes $[4]^{+}$ and $[5]^{+}$ the emission maxima depend significantly on the bidentate ligand, with a higher energy ($\lambda_{em}$ = 618 nm) for the less conjugated dppz complex, compared to dppn ($\lambda_{em}$ = 672 nm, see Table 3). Two results are apparently contradictory: the higher energy of the emitting ($^3MLCT$) excited states vs the very low calculated

and experimental $\Delta E$ values in $[4]^{+}$ and $[5]^{+}$, compared to $[1]^{+}$, $[2]^{+}$, and $[3]^{+}$. This contradiction suggests that the lower triplet states centered on dppz and dppn and arising from the photochemical population of the low-lying LUMO-like orbitals are not emissive; they are probably of $^3\pi-\pi^*$ character and centered on the phenazine moiety of the dppz or dppn ligand. The weakly emissive states, on the other hand, most likely of $^3MLCT$ character, are higher in energy in $[4]^{+}$ and $[5]^{+}$ because they are centered on the bpy moiety of dppz or dppn, while in $[1]^{+}$, $[2]^{+}$, and $[3]^{+}$ they are centered on the more conjugated phenyl-functionalized bipyridine ligand. All in all, the ligand photosubstitution reactions occur from metal-centered $^3MC$ states, which are high in energy for $[1]^{+}-[5]^{+}$ due to the excellent $\sigma$-donor properties of the cyclometalated ligand and probably poorly dependent on the conjugation of the bidentate ligand. Due to the presence of their low-lying $^3\pi-\pi^*$ states, $[4]^{+}$ and $[5]^{+}$ cannot perform any photosubstitution, as nonradiative decay pathways are faster.[42] For $[1]^{+}$, $[2]^{+}$, and $[3]^{+}$ these $^3\pi-\pi^*$ states are much higher in energy, so that the photogenerated, low-lying phbpy-based $^3MLCT$ states, in spite of the higher-lying $^3MC$ states, still leads to photosubstitution, though at a significantly lower rate than in the terpyridine analogue $[9]^{2+}$.

Chiral-at-metal complexes based upon ruthenium, iridium, or rhodium have been extensively investigated by the group of Meggers,[43−45] Barton,[46] and others[47−49] and have shown great promise in, e.g., asymmetric (photo)catalysis[50,51] or as anticancer drugs.[52] To resolve these types of complexes, a classical method consists of coordinating an enantiomerically pure chiral auxiliary to the metal center, resulting in a mixture of diastereomers which can be separated in preparative scales using normal phase chromatography such as silica.[53] After separation, these diastereoisomers are typically treated with an achiral monodentate ligand of interest, thus resolving the two pure enantiomers. Other resolution methods involve direct recrystallization of enantiomers using chiral counterions such

as Δ-TRISPHAT,[32,54−56] or separation of the enantiomers on chiral HPLC.[46] For [1]⁺−[5]⁺ these strategies could not be followed due on the one hand to the exceptional inertness of the coordination sphere and possibly to the very similar molecular shape of the cyclometalated vs. pyridyl side of the ruthenium-coordinated phbpy ligand. We hence relied on photochemical substitution to introduce a chiral sulfoxide ligand as resolving agent. The resulting diastereoisomeric ruthenium complexes [11-A]PF₆ and [11-C]PF₆ were inseparable on normal-phase silica. We therefore diverted to the use of reverse phase HPLC using 0.1% formic acid in the eluent. As a result, the isolation of the two diastereoisomers as their formate complexes was possible, but the presence of formic acid affected the overall yield (9%), most likely due to partial reprotonation of the cyclometalated ligand and subsequent (partial) degradation of the products. This is an issue that will be addressed in the future.

## CONCLUSION

Replacing the terpyridine tridentate ligand in [Ru(tpy)(NN)-L]²⁺ with phbpy has led to a new family of chiral-at-metal complexes [1]⁺−[5]⁺ with drastically altered thermal and photochemical properties compared to their polypyridine analogues. In particular, thermal substitution of the monodentate sulfoxide ligands becomes virtually impossible, while the ligand photosubstitution efficiency was reduced or even quenched due to the strong effect of cyclometalation on the energy of the HOMO and LUMO of the complexes. When N−N is a phenazine-based ligand ([4]⁺ or [5]⁺), the LUMO is based on the bidentate ligand and full quenching of the photoreactivity occurred, in great contrast to the photochemical behavior of terpyridine analogues such as [Ru(tpy)-(dppz)(SRR')]²⁺ or [Ru(tpy)(dppn)(SRR')]²⁺ that undergo selective photosubstitution in water ($\Phi_{450}$ = 0.02[27] and 0.00095,[36] respectively). The resolution of photosubstitutionally and thermally inert chiral cyclometalated complexes such as [4]⁺ and [5]⁺ will thus require strategies that still need to be developed. However, when N−N is bpy, phen, or dpq ([1]⁺−[3]⁺), selective photosubstitution of DMSO by acetonitrile remained possible. The ability of [1]⁺−[3]⁺ to exchange DMSO by acetonitrile upon visible light irradiation can be exploited, as demonstrated here with [2]⁺, to labilize the thermally inert achiral DMSO ligand and replace it in two steps by a chiral sulfoxide ligand, thus allowing the separation of the two chiral isomers [11-A]⁺ and [11-C]⁺. This works demonstrates that photosubstitution reactions can be useful for the resolution of chiral-at-metal organometallic complexes, which opens new synthetic routes toward catalytically or biologically active chiral organometallic complexes.

## ASSOCIATED CONTENT

**Ⓢ Supporting Information**

The Supporting Information is available free of charge on the ACS Publications website at DOI: 10.1021/jacs.8b10264.

> Synthetic procedures for the synthesis of [1]PF₆-[8]PF₆, [11-A/C]HCO₂, [12]−[16]; quantum yield determination for [1]PF₆, [2]PF₆, [3]PF₆, and [9]PF₆; NMR irradiation experiments for [1]PF₆−[3]PF₆; electrochemistry experiments; CD spectra for [11-A/C] HCO₂; DFT structures for [1]PF₆−[5]PF₆; and the NOESY spectrum of [11-A]HCO₂ (PDF)

> CIF files for the studied compounds (ZIP)

## AUTHOR INFORMATION

**Corresponding Author**
*bonnet@chem.leidenuniv.nl

**ORCID** ⊙
Sylvestre Bonnet: 0000-0002-5810-3657

**Author Contributions**
§These authors made an equal contribution to this work.

**Notes**
The authors declare no competing financial interest.

## REFERENCES

(1) Murray, B. S.; Babak, M. V.; Hartinger, C. G.; Dyson, P. J. The development of RAPTA compounds for the treatment of tumors. *Coord. Chem. Rev.* **2016**, *306*, 86−114.

(2) Dougan, S. J.; Sadler, P. J. The design of organometallic ruthenium arene anticancer agents. *Chimia* **2007**, *61* (11), 704−715.

(3) Pena, B.; David, A.; Pavani, C.; Baptista, M. S.; Pellois, J. P.; Turro, C.; Dunbar, K. R. Cytotoxicity Studies of Cyclometallated Ruthenium(II) Compounds: New Applications for Ruthenium Dyes. *Organometallics* **2014**, *33* (5), 1100−1103.

(4) Mari, C.; Pierroz, V.; Rubbiani, R.; Patra, M.; Hess, J.; Spingler, B.; Oehninger, L.; Schur, J.; Ott, I.; Salassa, L.; Ferrari, S.; Gasser, G. DNA intercalating Ru(II) polypyridyl complexes as effective photosensitizers in photodynamic therapy. *Chem. - Eur. J.* **2014**, *20* (44), 14421−36.

(5) Wachter, E.; Heidary, D. K.; Howerton, B. S.; Parkin, S.; Glazer, E. C. Light-activated ruthenium complexes photobind DNA and are cytotoxic in the photodynamic therapy window. *Chem. Commun.* **2012**, *48* (77), 9649−51.

(6) Chan, H.; Ghrayche, J. B.; Wei, J.; Renfrew, A. K. Photolabile Ruthenium (II)−Purine Complexes: Phototoxicity, DNA Binding, and Light-Triggered Drug Release. *Eur. J. Inorg. Chem.* **2017**, *2017* (12), 1679−1686.

(7) Burke, C. S.; Byrne, A.; Keyes, T. E. Highly Selective Mitochondrial Targeting by a Ruthenium(II) Peptide Conjugate: Imaging and Photoinduced Damage of Mitochondrial DNA. *Angew. Chem., Int. Ed.* **2018**, *57* (38), 12420−12424.

(8) Burke, C. S.; Byrne, A.; Keyes, T. E. Targeting Photoinduced DNA Destruction by Ru(II) Tetraazaphenanthrene in Live Cells by Signal Peptide. *J. Am. Chem. Soc.* **2018**, *140* (22), 6945−6955.

(9) Huisman, M.; White, J. K.; Lewalski, V. G.; Podgorski, I.; Turro, C.; Kodanko, J. J. Caging the uncageable: using metal complex release for photochemical control over irreversible inhibition. *Chem. Commun.* **2016**, *52* (85), 12590−12593.

(10) Li, A.; Yadav, R.; White, J. K.; Herroon, M. K.; Callahan, B. P.; Podgorski, I.; Turro, C.; Scott, E. E.; Kodanko, J. J. Illuminating cytochrome P450 binding: Ru(ii)-caged inhibitors of CYP17A1. *Chem. Commun.* **2017**, *53* (26), 3673−3676.

(11) Albani, B. A.; Pena, B.; Leed, N. A.; de Paula, N. A.; Pavani, C.; Baptista, M. S.; Dunbar, K. R.; Turro, C. Marked improvement in photoinduced cell death by a new tris-heteroleptic complex with dual action: singlet oxygen sensitization and ligand dissociation. *J. Am. Chem. Soc.* **2014**, *136* (49), 17095−101.

(12) Albani, B. A.; Pena, B.; Dunbar, K. R.; Turro, C. New cyclometallated Ru(II) complex for potential application in photochemotherapy? *Photochem. Photobiol. Sci.* **2014**, *13* (2), 272−80.

(13) Leyva, L.; Sirlin, C.; Rubio, L.; Franco, C.; Le Lagadec, R.; Spencer, J.; Bischoff, P.; Gaiddon, C.; Loeffler, J. P.; Pfeffer, M. Synthesis of cycloruthenated compounds as potential anticancer agents. *Eur. J. Inorg. Chem.* **2007**, *2007* (19), 3055–3066.

(14) Liu, J.; Ji, L. N.; Mei, W. J. The development of ruthenium complexes as anticancer drugs activation and anticancer mechanism. *PROG CHEM* **2004**, *16* (6), 969–974.

(15) Kreitner, C.; Erdmann, E.; Seidel, W. W.; Heinze, K. Understanding the Excited State Behavior of Cyclometalated Bis(tridentate)ruthenium(II) Complexes: A Combined Experimental and Theoretical Study. *Inorg. Chem.* **2015**, *54* (23), 11088–11104.

(16) Kreitner, C.; Heinze, K. The photochemistry of mono- and dinuclear cyclometalated bis(tridentate)ruthenium(II) complexes: dual excited state deactivation and dual emission. *Dalton Trans.* **2016**, *45* (13), 5640–58.

(17) Kreitner, C.; Heinze, K. Excited state decay of cyclometalated polypyridine ruthenium complexes: insight from theory and experiment. *Dalton Trans.* **2016**, *45* (35), 13631–47.

(18) Huang, H.; Zhang, P.; Chen, H.; Ji, L.; Chao, H. Comparison between polypyridyl and cyclometalated ruthenium(II) complexes: anticancer activities against 2D and 3D cancer models. *Chem. - Eur. J.* **2015**, *21* (2), 715–25.

(19) Schatzschneider, U.; Niesel, J.; Ott, I.; Gust, R.; Alborzinia, H.; Wolfl, S. Cellular uptake, cytotoxicity, and metabolic profiling of human cancer cells treated with ruthenium(II) polypyridyl complexes [Ru(bpy)2(N–N)]Cl2 with N–N = bpy, phen, dpq, dppz, and dppn. *ChemMedChem* **2008**, *3* (7), 1104–9.

(20) Mari, C.; Pierroz, V.; Ferrari, S.; Gasser, G. Combination of Ru(ii) complexes and light: new frontiers in cancer therapy. *Chem. Sci.* **2015**, *6* (5), 2660–2686.

(21) Funaki, T.; Yanagida, M.; Onozawa-Komatsuzaki, N.; Kasuga, K.; Kawanishi, Y.; Kurashige, M.; Sayama, K.; Sugihara, H. Synthesis of a new class of cyclometallated ruthenium(II) complexes and their application in dye-sensitized solar cells. *Inorg. Chem. Commun.* **2009**, *12* (9), 842–845.

(22) Palmer, A. M.; Pena, B.; Sears, R. B.; Chen, O.; El Ojaimi, M.; Thummel, R. P.; Dunbar, K. R.; Turro, C. Cytotoxicity of cyclometallated ruthenium complexes: the role of ligand exchange on the activity. *Philos. Trans. R. Soc., A* **2013**, *371* (1995), 20120135.

(23) Lin, Z.; Gong, L.; Celik, M. A.; Harms, K.; Frenking, G.; Meggers, E. Asymmetric coordination chemistry by chiral-auxiliary-mediated dynamic resolution under thermodynamic control. *Chem. - Asian J.* **2011**, *6* (2), 474–81.

(24) Gong, L.; Mulcahy, S. P.; Harms, K.; Meggers, E. Chiral-auxiliary-mediated asymmetric synthesis of tris-heteroleptic ruthenium polypyridyl complexes. *J. Am. Chem. Soc.* **2009**, *131* (28), 9602–3.

(25) Gong, L.; Wenzel, M.; Meggers, E. Chiral-auxiliary-mediated asymmetric synthesis of ruthenium polypyridyl complexes. *Acc. Chem. Res.* **2013**, *46* (11), 2635–44.

(26) Ryabov, A. D.; Le Lagadec, R.; Estevez, H.; Toscano, R. A.; Hernandez, S.; Alexandrova, L.; Kurova, V. S.; Fischer, A.; Sirlin, C.; Pfeffer, M. Synthesis, characterization, and electrochemistry of biorelevant photosensitive low-potential orthometalated ruthenium complexes. *Inorg. Chem.* **2005**, *44* (5), 1626–34.

(27) Lameijer, L. N.; Breve, T. G.; van Rixel, V. H. S.; Askes, S. H. C.; Siegler, M. A.; Bonnet, S. Effects of the Bidentate Ligand on the Photophysical Properties, Cellular Uptake, and (Photo)cytotoxicity of Glycoconjugates Based on the [Ru(tpy)(NN)(L)](2+) Scaffold. *Chem. - Eur. J.* **2018**, *24* (11), 2709–2717.

(28) Rack, J. J.; Winkler, J. R.; Gray, H. B. Phototriggered Ru(II)-dimethylsulfoxide linkage isomerization in crystals and films. *J. Am. Chem. Soc.* **2001**, *123* (10), 2432–3.

(29) Rachford, A. A.; Petersen, J. L.; Rack, J. J. Designing molecular bistability in ruthenium dimethyl sulfoxide complexes. *Inorg. Chem.* **2005**, *44* (22), 8065–75.

(30) Bonnet, S.; Collin, J. P.; Gruber, N.; Sauvage, J. P.; Schofield, E. R. Photochemical and thermal synthesis and characterization of

(31) polypyridine ruthenium(II) complexes containing different monodentate ligands. *Dalton Trans.* **2003**, *24*, 4654–4662.

(31) Goldbach, R. E.; Rodriguez-Garcia, I.; van Lenthe, J. H.; Siegler, M. A.; Bonnet, S. N-acetylmethionine and biotin as photocleavable protective groups for ruthenium polypyridyl complexes. *Chem. - Eur. J.* **2011**, *17* (36), 9924–9.

(32) Laleu, B.; Mobian, P.; Herse, C.; Laursen, B. W.; Hopfgartner, G.; Bernardinelli, G.; Lacour, J. Resolution of [4]heterohelicenium dyes with unprecedented Pummerer-like chemistry. *Angew. Chem., Int. Ed.* **2005**, *44* (12), 1879–83.

(33) Gottle, A. J.; Alary, F.; Boggio-Pasqua, M.; Dixon, I. M.; Heully, J. L.; Bahreman, A.; Askes, S. H.; Bonnet, S. Pivotal Role of a Pentacoordinate (3)MC State on the Photocleavage Efficiency of a Thioether Ligand in Ruthenium(II) Complexes: A Theoretical Mechanistic Study. *Inorg. Chem.* **2016**, *55* (9), 4448–56.

(34) Barigelletti, F.; Ventura, B.; Collin, J. P.; Kayhanian, R.; Gavina, P.; Sauvage, J. P. Electrochemical and spectroscopic properties of cyclometallated and non-cyclometallated ruthenium(II) complexes containing sterically hindering ligands of the phenanthroline and terpyridine families. *Eur. J. Inorg. Chem.* **2000**, *2000* (1), 113–119.

(35) Collin, J. P.; Beley, M.; Sauvage, J. P.; Barigelletti, F. A Room-Temperature Luminescent Cyclometallated Ruthenium(Ii) Complex of 6-Phenyl-2,2'-Bipyridine. *Inorg. Chim. Acta* **1991**, *186* (1), 91–93.

(36) Lameijer, L. N.; Hopkins, S. L.; Breve, T. G.; Askes, S. H.; Bonnet, S. d- Versus l-Glucose Conjugation: Mitochondrial Targeting of a Light-Activated Dual-Mode-of-Action Ruthenium-Based Anti-cancer Prodrug. *Chem. - Eur. J.* **2016**, *22* (51), 18484–18491.

(37) Knoll, J. D.; Albani, B. A.; Durr, C. B.; Turro, C. Unusually efficient pyridine photodissociation from Ru(II) complexes with sterically bulky bidentate ancillary ligands. *J. Phys. Chem. A* **2014**, *118* (45), 10603–10.

(38) Jang, H. J.; Hopkins, S. L.; Siegler, M. A.; Bonnet, S. Frontier orbitals of photosubstitutionally active ruthenium complexes: an experimental study of the spectator ligands' electronic properties influence on photoreactivity. *Dalton Trans.* **2017**, *46* (30), 9969–9980.

(39) Rack, J. J.; Rachford, A. A.; Shelker, A. M. Turning off phototriggered linkage isomerizations in ruthenium dimethyl sulfoxide complexes. *Inorg. Chem.* **2003**, *42* (23), 7357–9.

(40) Foxon, S. P.; Metcalfe, C.; Adams, H.; Webb, M.; Thomas, J. A. Electrochemical and photophysical properties of DNA metallo-intercalators containing the ruthenium(II) tris(1-pyrazolyl)methane unit. *Inorg. Chem.* **2007**, *46* (2), 409–16.

(41) White, T. A.; Maji, S.; Ott, S. Mechanistic insights into electrocatalytic CO 2 reduction within [Ru II (tpy)(NN) X ] n+ architectures. *Dalton Trans.* **2014**, *43* (40), 15028–15037.

(42) Knoll, J. D.; Albani, B. A.; Turro, C. New Ru(II) complexes for dual photoreactivity: ligand exchange and (1)O2 generation. *Acc. Chem. Res.* **2015**, *48* (8), 2280–7.

(43) Huo, H.; Shen, X.; Wang, C.; Zhang, L.; Rose, P.; Chen, L. A.; Harms, K.; Marsch, M.; Hilt, G.; Meggers, E. Asymmetric photoredox transition-metal catalysis activated by visible light. *Nature* **2014**, *515* (7525), 100–3.

(44) Tan, Y.; Yuan, W.; Gong, L.; Meggers, E. Aerobic Asymmetric Dehydrogenative Cross-Coupling between Two C(sp3)-H Groups Catalyzed by a Chiral-at-Metal Rhodium Complex. *Angew. Chem., Int. Ed.* **2015**, *54* (44), 13045–8.

(45) Meggers, E. Asymmetric Synthesis of Octahedral Coordination Complexes. *Eur. J. Inorg. Chem.* **2011**, *2011* (19), 2911–2926.

(46) Boyle, K. M.; Barton, J. K. A Family of Rhodium Complexes with Selective Toxicity toward Mismatch Repair-Deficient Cancers. *J. Am. Chem. Soc.* **2018**, *140* (16), 5612–5624.

(47) Li, Z. Z.; Wen, A. H.; Yao, S. Y.; Ye, B. H. Enantioselective syntheses of sulfoxides in octahedral ruthenium(II) complexes via a chiral-at-metal strategy. *Inorg. Chem.* **2015**, *54* (6), 2726–33.

(48) Hesek, D.; Inoue, Y.; Ishida, H.; Everitt, S. R. L.; Drew, M. G. B. The first asymmetric synthesis of chiral ruthenium tris(bipyridine) from racemic ruthenium bis(bipyridine) complexes. *Tetrahedron Lett.* **2000**, *41* (15), 2617–2620.

(49) Hesek, D.; Inoue, Y.; Everitt, S. R. L.; Ishida, H.; Kunieda, M.; Drew, M. G. B. Conversion of a new chiral reagent Δ-[Ru(bpy)2 (dmso)Cl]PF6 to Δ-[Ru(bpy)2(dmbpy)]PF6Cl with 96.8% retention of chirality (dmbpy = 4,4′-dimethyl-2,2′-bipyridine). *Chem. Commun.* **1999**, No. 5, 403−404.

(50) Huo, H.; Fu, C.; Harms, K.; Meggers, E. Asymmetric catalysis with substitutionally labile yet stereochemically stable chiral-at-metal iridium(III) complex. *J. Am. Chem. Soc.* **2014**, *136* (8), 2990−3.

(51) Ma, J.; Shen, X.; Harms, K.; Meggers, E. Expanding the family of bis-cyclometalated chiral-at-metal rhodium(iii) catalysts with a benzothiazole derivative. *Dalton Trans.* **2016**, *45* (20), 8320−3.

(52) Wang, Y.; Huang, H.; Zhang, Q.; Zhang, P. Chirality in metal-based anticancer agents. *Dalton Trans.* **2018**, *47* (12), 4017−4026.

(53) Helms, M.; Lin, Z. J.; Gong, L.; Harms, K.; Meggers, E. Method for the Preparation of Nonracemic Bis-Cyclometalated Iridium(III) Complexes. *Eur. J. Inorg. Chem.* **2013**, *2013* (24), 4164−4172.

(54) Lacour, J.; Ginglinger, C.; Grivet, C.; Bernardinelli, G. Synthesis and Resolution of the Configurationally Stable Tris-(tetrachlorobenzenediolato)phosphate(V) Ion. *Angew. Chem., Int. Ed. Engl.* **1997**, *36* (6), 608−610.

(55) Lacour, J.; Jodry, J. J.; Ginglinger, C.; Torche-Haldimann, S. Diastereoselective Ion Pairing of TRISPHAT Anions and Tris(4,4′-dimethyl-2,2′-bipyridine)iron(II). *Angew. Chem., Int. Ed.* **1998**, *37* (17), 2379−2380.

(56) Lacour, J.; Goujon-Ginglinger, C.; Torche-Haldimann, S.; Jodry, J. Efficient Enantioselective Extraction of Tris(diimine)-ruthenium(II) Complexes by Chiral, Lipophilic TRISPHAT Anions. *Angew. Chem., Int. Ed.* **2000**, *39* (20), 3695−3697.